

RESEARCH PAPER



## Characterization of a novel allele encoding pheophorbide a oxygenase in rice

Zhihong Zhang, Yan He, Liangjian Li, Xiaobo Zhang, Xia Xu, Yongfeng Shi, and Jian-Li Wu 

State Key Laboratory of Rice Biology, China National Rice Research Institute, Hangzhou, China

### ABSTRACT

We identified a *rapid cell death 2* (*rcd2*) mutant from an indica cultivar Zhongjian100 mutant bank. The red-brown lesions appeared firstly on young seedling leaves, then gradually merged and the leaves completely withered at the late tillering stage. *rcd2* displayed apparent cell death at/around the lesions, accumulation of superoxide anion ( $O_2^-$ ) and disturbed ROS scavenging system, impaired photosynthetic capacity with significantly reduced chlorophyll content. The lesion formation was controlled by a single recessive nuclear gene and induced by natural light as well as mechanical wounding. A single base mutation (A1726T) at the 6th exon of *OsMH\_03G0040800* resulted in I576F substitution in the encoding protein, pheophorbide a oxygenase (PAO). Functional complementation could rescue the mutant phenotype and PAO-knockout lines exhibited the similar phenotype to *rcd2*. The activity of PAO decreased significantly while the content of PAO substrate, pheophorbide a, increased apparently in *rcd2*. The expression of chlorophyll synthesis/degradation-related genes and the contents of metabolic intermediates were largely changed. Furthermore, the level of chlorophyllide a, the product of chlorophyllase, increased significantly, indicating chlorophyllase might play a role in chlorophyll degradation in rice. Our results suggested that the I576F substitution disrupted PAO function, leading to  $O_2^-$  accumulation and chlorophyll degradation breakdown in rice.

### ARTICLE HISTORY

Received 10 November 2020  
Revised 9 December 2020  
Accepted 10 December 2020

### KEYWORDS

Rice; cell death;  
pheophorbide a oxygenase;  
chlorophyll; chlorophyllase

## Introduction

One of the most obvious signs of plant senescence is the loss of green color, that is, the degradation of chlorophyll (Chl), which is of great significance for plant growth, development and reproduction. Chl degradation is catalyzed by a series of Chl catabolic enzymes (CCEs) among which pheophorbide a oxygenase (PAO) is the key enzyme in the pathway termed the “PAO” pathway.<sup>1</sup>

During the process, the intermediate, pheophorbide (Pheide) a, is further converted into red Chl catabolite (RCC) by the catalysis of PAO and begin to the next step of degradation.<sup>2,3</sup> It has been commonly observed that PAO mutants from multiple plant species including the maize *lethal leaf spot 1* (*lls1*), Arabidopsis *accelerated cell death 1* (*acd1*), rice *early senescence 1* (*eas1*), sorghum *dropdead1* (*ded1*), tomato virus-induced gene silencing PAO mutants, and wheat PAO ortholog knockdown mutants result in necrotic lesion formation.<sup>4–10</sup> In fact, the protein sequence are highly conserved with a similarity up to 70% manifested by a conserved N-terminal chloroplast transit peptide sequence among plant species such as Arabidopsis, tomato, corn and rapeseed.<sup>11</sup> In rice, EAS1 is 68% identical to Arabidopsis ACD1. Unlike ACD1 that contains a single transit peptide, EAS1 contains two putative transit peptides in the N-terminus, suggesting that the targeting of EAS1 to chloroplasts is likely mediated by a putative bipartite transit peptide.<sup>9</sup> Whether it is a unique mechanism for PAO transport into the chloroplasts in monocot has yet to be clarified. So far, it is generally considered that the reason for lesion formation in PAO mutants is conserved across plant species due to a common fact that the metabolic defect universally induces the burst of reactive oxygen species (ROS) and subsequent cell death.<sup>10</sup> It has been noticed that the blocking of PAO activity in these

mutants may accumulate a phototoxic catabolic intermediate that produces singlet oxygen in light [Mach. 2001]. In maize, LLS1 is a chloroplast-localized protein and may act to prevent ROS formation or serve to remove a cell death mediator so as to maintain chloroplast integrity and cell survival.<sup>7,12</sup> In Arabidopsis, the delayed cell death phenotype of *acd1* in darkness may be in part explained by a lower production of  $H_2O_2$  or other ROS in the mutant plants that are expected to exhibit reduced photorespiration and the Mehler reaction.<sup>7</sup> In sorghum, the lack of superoxide anion and  $H_2O_2$  production at/around lesions suggests these two ROSs are not responsible for lesion formation in *ded1*; instead, singlet oxygen ( $^1O_2$ ) might be the direct cause but has yet to be clarified.<sup>10</sup> Besides, the lesions of *lls1*, *acd1* and *ded1* all appear on the leaves at the late growing stage, conferring severe impacts on plant reproductive growth. Overall, the direct cause for lesion formation in many lesion mimic/spotted-leaf mutants is largely controversial and required further studies.

Unlike PAO, the role of chlorophyllase (CLH), which could catalyze the hydrolysis of Chl to chlorophyllide (Chlide) and phytol, has long been considered to participate in the first step of Chl degradation [Takamiya et al. 2000; Harpaz-Saad et al. 2007].<sup>13,14</sup> However, some CLHs do not have a chloroplast transit peptide, indicating the involvement of other enzymes rather than CLH or presence of alternative pathways outside the chloroplasts.<sup>13,15</sup> In addition, Arabidopsis mutants with interrupted expression of either *AtCLH1* and *AtCLH2* or both of them are able to degrade Chl during senescence. Both CLHs localize to the cytosol when tagged with the green fluorescent protein, suggesting that CLHs are not essential for Chl degradation in Arabidopsis.<sup>16</sup> In contrast, antisense-suppression of broccoli CLH could delay the he

**CONTACT** Jian-li Wu  [beishangd@163.com](mailto:beishangd@163.com)  State Key Laboratory of Rice Biology China National Rice Research Institute, Hangzhou 310006, China.

 Supplemental data for this article can be accessed on the [publisher's website](#).

© 2020 The Author(s). Published with license by Taylor & Francis Group, LLC.

This is an Open Access article distributed under the terms of the Creative Commons Attribution-NonCommercial-NoDerivatives License (<http://creativecommons.org/licenses/by-nc-nd/4.0/>), which permits non-commercial re-use, distribution, and reproduction in any medium, provided the original work is properly cited, and is not altered, transformed, or built upon in any way.

ad yellowing rate after harvest.<sup>17</sup> The lemon CLH is localized to the chloroplast as shown by in situ immunofluorescence and is co-purified with chloroplast membranes after heterologous expression in tobacco mesophyll protoplasts.<sup>2</sup> Furthermore, it has been shown that CLH participates in Chl breakdown during fruit ripening in Citrus species as the cellular Chl quantity is negatively correlated with plastid CLH accumulation, i.e. plastids with reduced Chl content contains significant levels of CLH, while plastids containing still-intact chlorophyll lack any CLH signal.<sup>14,18</sup> Therefore, the role of CLH in Chl degradation remains to be clarified in plants. As one of the most important monocot species, the role of CLH in Chl degradation remains elusive in rice.

We report here the identification of a *rapid cell death 2 (rcd2)* mutant with deficient PAO resulting from a single amino acid substitution at position 576 (I/F). Furthermore, we found that the accumulation of superoxide anion ( $O_2^-$ ) instead of hydrogen peroxide ( $H_2O_2$ ) is likely responsible for the cell death in *rcd2* and CLHs might play a role in Chl degradation in rice.

## Materials and methods

### Rice materials

The *rcd2* mutant was originated from ethane methyl sulfonate (EMS) induced indica cultivar Zhongjian100 (wild type, WT). The rapid cell death phenotype has been stably inherited over multiple generations under the field and greenhouse conditions in Fuyang, Hangzhou, Zhejiang Province, China and Lingshui, Hainan Province, China. The mutant was used as the female parent and crossed, respectively, with the normal green leaf variety 80A90YR72 and Nipponbare to generate two  $F_2$  populations. The parents and the  $F_2$  individuals were grown in the paddy field at the China National Rice Research Institute (CNRRI) for genetic analysis and gene mapping. The complementary lines and the CRISPR/Cas9-mediated knockout lines derived from Kitaake were grown in the greenhouse at CNRRI.

### Agronomic trait evaluation

The mutant *rcd2* and the wild-type were grown in the paddy field at CNRRI from May to October 2018 with a conventional management of water and fertilizer. The major agronomic traits including plant height, internode length, number of tillers per plant, panicle length, number of filled grains per panicle, seed-setting rate and 1000-grain weight were measured from three-randomly chosen individual plants at full maturity. The means from three replicates were used for analysis by Student's *t*-test with the Excel 2016 software.

### Histochemical analysis

The WT leaves and *rcd2* leaves with lesions at the tillering stage were collected for histochemical assay. Cell death was detected by

trypan blue staining according to Yin et al.<sup>19</sup> Furthermore, the leaf samples were also used for a terminal deoxyribo-nucleotidyl transferase-mediated dUTP nick-end labeling (TUNEL) assay by using a Fluorescein in situ Cell Death Detection Kit following the manufacturer's instructions (Roche, Basel, Switzerland). Samples were photographed using a confocal laser scanning microscope (Ceise, Jena, Germany). The hydrogen peroxide ( $H_2O_2$ ) accumulation was detected by 3,3'-diaminobenzidine (DAB) staining.<sup>20</sup> Superoxide anion ( $O_2^-$ ) accumulation was detected by nitroblue tetrazolium (NBT) staining according to the method described by Qiao et al.<sup>21</sup> The pictures were recorded using a scanner (HP scanner jet 4010, Shanghai, China).

## Genetic analysis and gene mapping

The  $F_1$  plants were grown in the paddy field at CNRRI for determining the dominant/recessive nature of the target gene(s). The  $F_2$  individuals were used for segregation analysis and gene mapping. Bulk segregant analysis was first used to rapidly locate the mutation on a chromosome and a physical linkage map was then constructed using additional markers surrounding the mutation. Equal amounts of leaves from 20 plants of 80A90YR72 (the male parent) and 20 *rcd2* plants were collected for DNA extraction to form a wild-type DNA pool and a mutant-type DNA pool, respectively. The DNA of the parents and  $F_2$  individuals with mutant phenotype were extracted following the method of Edwards et al.<sup>22</sup> Simple sequence repeat (SSR) markers were obtained from the website (<http://www.gramene.org/>) while insertion/deletion (InDel) markers were designed using the Primer 5.0 software after comparison of the sequences between the japonica cultivar Nipponbare and the indica cultivar 93-11 on the website (<http://plants.ensembl.org/index.html>, [http://gramene.org/genome\\_browser/index.html](http://gramene.org/genome_browser/index.html)). PCR was performed in a total volume of 10  $\mu$ L reaction buffer containing 50 ng template DNA, 1.0  $\mu$ mol/L each primer, 5.0  $\mu$ L of 2  $\times$  PCR mixture (TsingKe Biological Technology, Hangzhou, China). The reaction was performed on a Biometra Thermal Cycler (Hiomedizinische Analytik, Germany): Pre-denaturation at 94°C for 2 min, followed by 35 cycles of 94°C for 30 s, 55°C for 30 s and 72°C for 30 s, with a final extension at 72°C for 5 min. The PCR products were run on 6% non-denaturing polyacrylamide gel electrophoresis (PAGE) and detected using silver staining. The primers were synthesized by TsingKe Biological Technology (Hangzhou, China). The primers for gene mapping are listed in Supplemental Table 1.

### Shading and dark treatment

To determine the effect of natural light on the initiation of lesions, the leaf shading experiment was carried out at the tillering stage. The top second leaves without lesions in *rcd2* and WT were shaded, respectively, with a piece of 1–2 cm aluminum foil for 4 d under natural field conditions. Then, the foil was removed and

**Table 1.** Comparison of agronomic traits between WT and *rcd2*.

Material	Plant height (cm)	Panicle length (cm)	No. tiller per plant	No. filled grain per panicle	Seed-setting rate (%)	1000-grain weight (g)
WT	116.7 $\pm$ 1.53	21.64 $\pm$ 3.08	14.5 $\pm$ 2.48	186.70 $\pm$ 17.69	85.45 $\pm$ 0.62	21.52 $\pm$ 0.42
<i>rcd2</i>	78.0 $\pm$ 1.73**	20.51 $\pm$ 2.70*	11.0 $\pm$ 1.73**	101.67 $\pm$ 5.13**	76.38 $\pm$ 2.68**	17.99 $\pm$ 0.23**

Values are means  $\pm$  SD; *n* = 3; \* indicates significance at  $P \leq 0.05$ ; \*\* indicates high significance at  $P \leq 0.01$  by Student's *t*-test.

light was reinstated for 3–7 d. Lesion development was photographed by a scanner (HP scanner jet 4010, Shanghai, China). To investigate the influence of dark on the leaf color and Chl content, the detached leaves of *rcd2* without lesions and WT at the tillering stage were cut into 2 cm pieces, and placed in Petri dishes filled with water in dark at room temperature for 8 d. Means of Chl content from three replicates were used for analysis by Student's *t*-test.

### RNA extraction and gene expression analysis

Total RNA was extracted from leaves of *rcd2* and WT using NucleoZOL Reagent Kit according to the manufacturer's instructions (Macherey-Nagel, Düren, Germany). RNA was reverse-transcribed using the ReverTra Ace qPCR RT Master Mix with genomic DNA (gDNA) Remover Kit (Toyobo, Osaka, Japan). The quantitative real-time PCR (qRT-PCR) was carried out using the FastStar Essential DNA Green Master Kit (Roche, Basel, Switzerland) and performed on a Thermal Cycler Dice Real Time System II (Takara, Kusatsu, Japan), following the method described previously.<sup>22</sup> The rice *Ubiquitin* was used as the internal control to normalize expression levels. The means from three replicates were used for analysis by Student's *t*-test with the Excel 2016 software. All primers used in qRT-PCR are listed in Supplemental Table 1.

### Determination of enzyme activity and substrate content

At the tillering stage, 0.5 g fresh weight of the top second leaves from WT and *rcd2* under filed and dark conditions were used to determine the contents of enzymes and relevant substrates. The activity of enzymes associated with Chl degradation and the content of substrates were determined by the ELISA Kits (MEIMI AN, Suzhou, China) following the manufacturer's instructions. The kits and catalog numbers are as follows: PAO content (MM-6255501), PAO activity (RJ25335), Pheide a content (MM-3297102), Chlide a content (MM-6256602), Phein a content (MM-6256402), CLH activity (MM-089001), PPH activity (MM-252601), RCCR activity (MM-6254801), MDCase activity (MM-6255001). The absorbance was collected by using a SpectraMax i3x multi-mode microplate reader (Molecular Devices).

### Malonaldehyde (MDA), soluble protein contents and ROS-related parameter measurement

The leaf blades from WT and *rcd2* at the tillering stage were sampled and immediately frozen in liquid nitrogen. The activities of reactive oxygen species (ROS) scavenging enzymes, including peroxidase (POD), superoxide dismutase (SOD), and catalase (CAT), as well as the contents of malonaldehyde (MDA), hydrogen peroxide (H<sub>2</sub>O<sub>2</sub>) and soluble proteins (SP), were determined following the manufacturer's instructions (Nanjing Jiancheng Bioengineering Institute, Nanjing, China).

### Functional complementation and CRISPR/Cas9 knockout

The 6693 bp genomic DNA sequence containing a 4589 bp coding sequence, a 1600 bp upstream and a 504 bp downstream sequence was amplified from WT and inserted into the pCAMBIA1300 vector to generate a new construct pPAO-com for functional com

plementation. The CRISPR/Cas9 constructs were generated according to a previous report under the japonica cultivar 'Kitaake' background.<sup>23</sup> The pPAO-com and CRISPR/Cas9 constructs were introduced into the *Agrobacterium tumefaciens* strain EHA105 by electroporation and transformed, respectively, into the embryogenic calli derived from *rcd2* and Kitaake via *Agrobacterium tumefaciens*-mediated plant transformation.<sup>24</sup> All primers used are listed in Supplemental Table 1.

## Results

### Phenotypic characterization of *rcd2*

Under the natural field conditions, *rcd2* exhibited reddish-brown lesions at the bottom leaves approximately 14 d after sowing (Figure 1(a)). The new leaves were normal green similar to WT until 50d after sowing, and subsequently the reddish-brown lesions appeared from the bottom to the top on all the leaves. The lesions then merged and some leaves withered completely at both the tillering and heading stages (Figure 1(b,c)). Under the paddy field conditions, performance of agronomic traits including plant height, internode length, panicle length, number of tillers per plant, number of filled grains per panicle, seed-setting rate and 1000-grain weight were significantly decreased in *rcd2* compared with WT (Table 1). The shortened plant height was due to significantly reduced lengths of the third and fourth internodes (Figure 1(d)). Taken together, the mutation resulted in lesion formation and the poor performance of agronomic traits.

### Physiological alterations of *rcd2*

To determine the mutation effect on Chl metabolism, we firstly measured the Chl contents at the seedling and tillering stages. The results showed that the contents of Chl were similar between *rcd2* and WT at the seedling stage (four-leaf stage) when the lesions appeared only at the bottommost leaves. In contrast, the content of Chl was significantly lower than that of WT at the tillering stage when the lesions appeared on all the leaves of *rcd2* (Figure 1(e)). The results indicated that the formation of lesions significantly decreased the Chl level in *rcd2*.

We then examined the photosynthetic parameters and found that the net photosynthetic rate (P<sub>n</sub>), stomatal conductance (G<sub>s</sub>), transpiration rate (Tr) in *rcd2* were significantly lower than those of WT while the intercellular CO<sub>2</sub> concentration (C<sub>i</sub>) was apparently higher than that of WT in the uppermost leaves without lesions at the tillering stage (Table 2). The results indicated that the mutation resulted in significant decline of photosynthetic capacity in *rcd2*.

### ROS accumulation with perturbed ROS scavenging system and cell death in *rcd2*

To determine the direct cause for the rapid cell death phenotype, we carried out histochemical staining with *rcd2* and WT leaves. Trypan blue staining, an indicator of irreversible membrane damage or cell death,<sup>27</sup> showed that blue stains were observed in *rcd2* leaves, whereas no blue stains were observed on WT leaves (Figure 2(a)). To further confirm the membrane damage and cell death, we measured the levels of

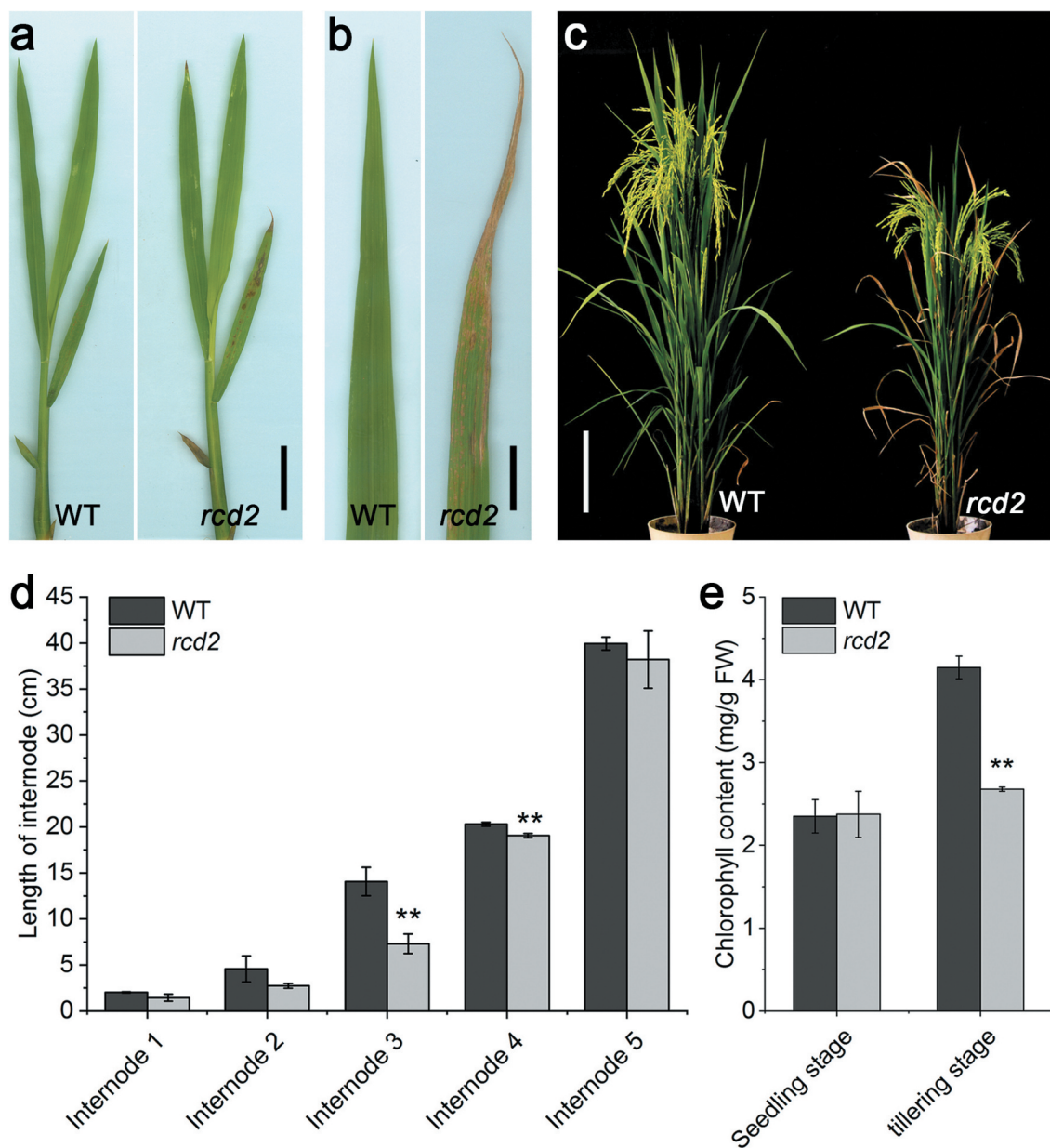


**Figure 1. Phenotypic characterization of *rcd2*.** (a) Phenotype at the four-leaf stage. Bar = 5 cm; (b) the top second leaves of wild type (WT) and *rcd2* at the tillering stage; Bar = 2 cm; (c) phenotypes of WT and *rcd2* at the heading stage. Bar = 20 cm; (d) internode length of the main stem at the mature stage in WT and *rcd2*; (e) Chl contents of WT and *rcd2*. Values are means  $\pm$  SD ( $n = 3$ ), \*\* indicates significance at  $P \leq 0.01$  by Student's *t*-test.

**Table 2.** Comparison of photosynthetic parameters between WT and *rcd2*.

Material	Pn ( $\mu\text{mol CO}_2\cdot\text{m}^{-2}\cdot\text{s}^{-1}$ )	Gs ( $\text{mol H}_2\text{O}\cdot\text{m}^{-2}\cdot\text{s}^{-1}$ )	Ci ( $\mu\text{mol CO}_2\cdot\text{mol}^{-1}$ )	Tr ( $\text{mmol H}_2\text{O}\cdot\text{m}^{-2}\cdot\text{s}^{-1}$ )
WT	23.97 $\pm$ 1.63	0.96 $\pm$ 0.03	312.09 $\pm$ 6.33	9.64 $\pm$ 0.80
<i>rcd2</i>	10.74 $\pm$ 0.23**	0.70 $\pm$ 0.07*	348.94 $\pm$ 5.24**	7.15 $\pm$ 0.55*

Values are means  $\pm$  SD;  $n = 3$ ; \* indicates significance at  $P \leq 0.05$ , \*\* indicates significance at  $P \leq 0.01$  by Student's *t*-test.

malonaldehyde (MDA) and soluble proteins (SP), and carried out TUNEL assay. The results showed that the MDA level was apparently higher and the SP level was significantly lower than those of WT at the tillering stage (Figure 2(d,e)). In addition, a large number of labeled nuclei (green) were detected as TUNEL positive signals in *rcd2*, whereas a few number of labeled nuclei were found in WT (Figure 2(f)), indicating the presence of increased DNA fragmentation in *rcd2*. Taken together, these results revealed that cell death occurred in *rcd2*.

Furthermore, to know whether the occurrence of cell death in *rcd2* was associated with the burst of ROS, we firstly carried out DAB staining and measured the level of  $\text{H}_2\text{O}_2$ . The results indicated that no red brown precipitates were observed both on *rcd2* and WT leaves at the tillering stage, and the  $\text{H}_2\text{O}_2$  content of *rcd2* was even lower than that of WT (Figure 2(b,g)). We then performed the NBT staining, an indicator of  $\text{O}_2^-$  accumulation, and the results showed that a large number of blue stains were observed in *rcd2* compared with WT (Figure 2(c)).

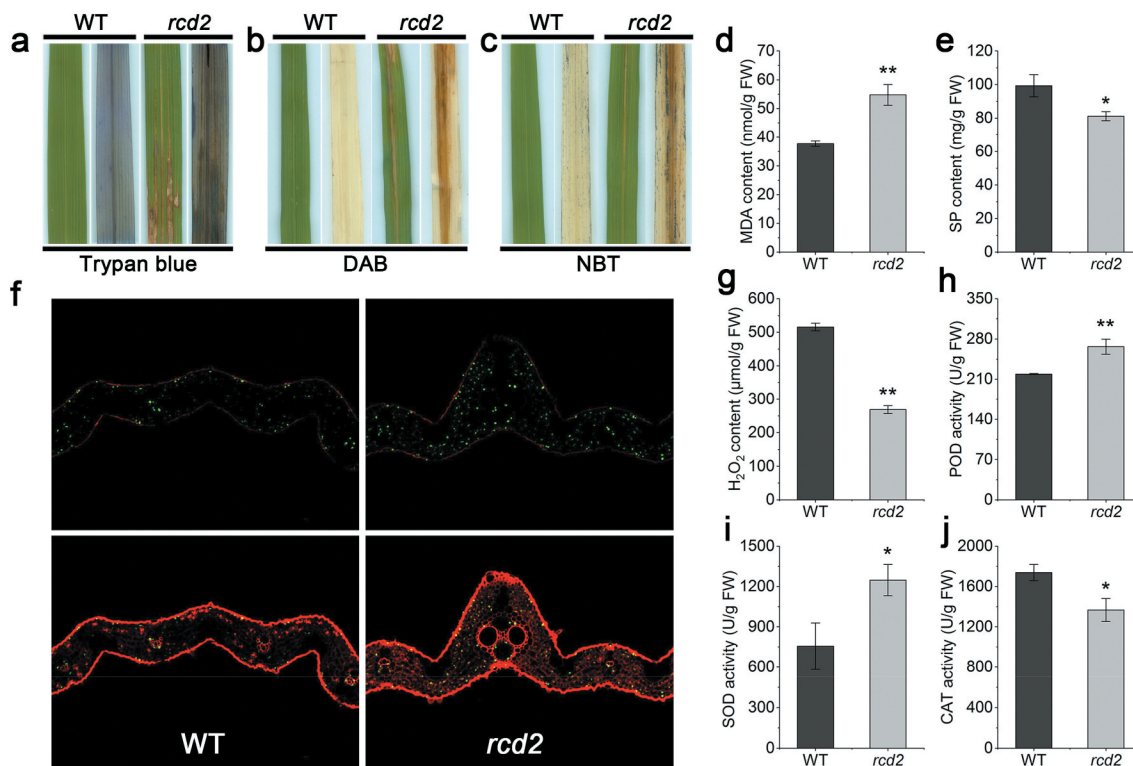


**Figure 2. Histochemical, TUNEL and ROS scavenging enzyme analysis.** (a-c) Trypan blue staining, DAB assay and NBT assay in WT and *rcd2* at the tillering stage. Bar = 2 cm; (d) malonaldehyde (MDA) contents of WT and *rcd2*; (e) soluble protein (SP) content of WT and *rcd2*; (f) TUNEL assay of WT and *rcd2* at the tillering stage. Green color represents positive result. (g) H<sub>2</sub>O<sub>2</sub> content of WT and *rcd2*; (h-j) superoxide dismutase (SOD) activity (h), peroxidase (POD) activity (i) and catalase (CAT) activity (j) of WT and *rcd2* at the tillering stage. Values are means ± SD; n = 3; \* indicates significance at  $P \leq 0.05$ ; \*\* indicates significance at  $P \leq 0.01$  by Student's *t*-test. The top second leaves at the tillering stage were used for analysis in all experiments.

These results indicated that the occurrence of cell death was probably associated with the burst of O<sub>2</sub><sup>-</sup> in *rcd2*.

Finally, to determine whether the accumulation of O<sub>2</sub><sup>-</sup> was associated with a perturbed ROS scavenging system, we measured the activities of ROS scavenging enzymes including peroxidase (POD), superoxide dismutase (SOD) and catalase (CAT). The results indicated that the activities of SOD and POD in *rcd2* leaves at the tillering stage were significantly higher than those of WT. In contrast, the activity of CAT was significantly lower than that of WT at the tillering stage (Figure 3(h-j)). The results suggested that the ROS scavenging system was apparently impaired and the excessive accumulation of O<sub>2</sub><sup>-</sup> that was likely responsible for the cell death in *rcd2*.

### Light-induced lesion formation and dark induced stay-green in *rcd2*

Lesion initiation of many mutants is light-dependent.<sup>25</sup> To determine the effect of light on *rcd2* lesion formation under field conditions, the leaves of *rcd2* without lesions and WT were covered with a piece of 2 cm aluminum foil for 4d. The results showed that the reddish-brown lesions did not appear in the shaded leaf area, while a mass of lesions emerged in the unshaded leaf area of *rcd2*. After removing the foil and reinstating the light for 5d, new reddish-brown lesions occurred in the shaded leaf area of *rcd2* (Figure 3(a)). These results suggested that the lesion initiation and development in *rcd2* were light-dependent. Furthermore, new reddish-brown lesions occurred in the leaves

of *rcd2* after mechanical wounding for 7d (Figure 3(b)), suggesting that the lesions could be induced by wounding as well.

It is well known that darkness could induce chlorosis and senescence in plants.<sup>26</sup> To determine whether the mutation could accelerate or delay senescence in darkness, the detached leaves were treated in dark for 8 d. The results showed that the detached leaves of *rcd2* could stay green longer than that of WT, and the Chl content in *rcd2* declined much slower than that of WT (Figure 3(c,d)). The results clearly showed that *rcd2* exhibited a retarded Chl degradation and “stay-green” phenotype in dark.

### Map-based isolation of *rcd2*

To determine the inheritance pattern of the *rcd2* phenotype, we crossed *rcd2* with three normal green leaf cultivars, including the wild-type, Nipponbare and 80A90YR72. All F<sub>1</sub> plants derived from the three crosses exhibited the normal green phenotype similar to WT, suggesting that the mutation was recessive in nature. In the population derived from *rcd2*/Nipponbare, 367 individuals exhibited normal phenotype, while 119 individuals exhibited mutant phenotype. The segregation of WT/mutant type fitted to the 3:1 Mendelian ratio ( $\chi^2 = 0.57 < \chi^2_{0.05} = 3.84$ ). Similarly, in the other two populations, the WT/mutant type segregation ratios were all fitted to 3:1 (Table 3). The results indicated that the *rcd2* phenotype was controlled by a single recessive gene. We then proceeded to map the mutation using the F<sub>2</sub> population derived from *rcd2*/

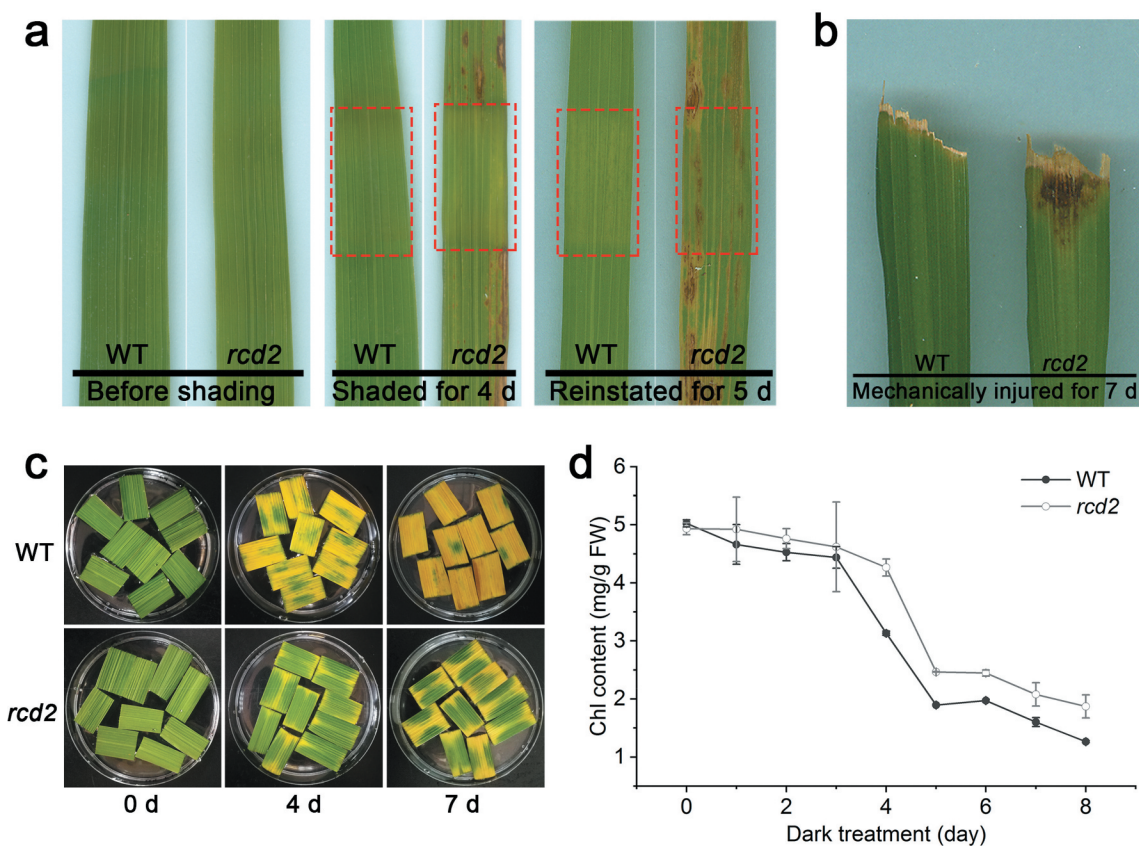


**Figure 3. Response of *rcd2* to light, wounding and darkness treatment.** (a) Effect of light on lesion formation in *rcd2*, including before shading, shaded for 4 d and reinstated for 5 d. The red dotted line box indicates the shaded area. Bar = 1 cm; (b) effect of mechanical wounding on lesion formation in *rcd2*. Bar = 1 cm; (c) detached *rcd2* leaves stayed green under dark conditions. Bar = 1 cm; (d) the chlorophyll (Chl) contents measured at 1–8 d after dark treatment. Values are means  $\pm$  SD;  $n=3$ .

**Table 3.** Genetic analysis of *rcd2*.

Cross	Phenotype $F_1$	$F_2$ Total no. of plants		$P_{(3:1)}$	$\chi^2_{0.05}$
		No. of WT plants	No. of mutant-type plants		
<i>rcd2</i> /Nipponbare	Green leaf	486	119	0.79	0.07
<i>rcd2</i> /80A90YR72	Green leaf	2938	748	0.57	0.33
<i>rcd2</i> /wild type	Green leaf	176	133	0.86	0.03

80A90YR72 by bulk segregation analysis. Two markers RM22 and RM14641 on chromosome 3 were identified to be linked to the mutation in an initial mapping (Figure 4(a)). To fine map the locus, 893  $F_2$  individuals with *rcd2* phenotype were genotyped and the mutation was finally delimited to a 145 kb interval between markers InDel11 and InDel16 (Figure 4(a)). The WT DNA and the *rcd2* DNA were subjected to high throughput sequencing, and the results showed that a single nucleotide substitution from A to T at position 1726 was detected between WT and *rcd2* in the 145 kb candidate region (Figure 4(a)). The A1726T substitution localizes to the 6th exon of *OsMH\_03G0040800*, leading to the change from isoleucine to phenylalanine at position 576 in the putative coding protein (Figure 4(b)). The results indicated that *OsMH\_03G0040800* was likely the candidate gene responsible for the mutant trait.

To confirm whether *OsMH\_03G0040800* was the target gene, we carried out functional complementation. The construct pPAO-com carrying the WT allele was introduced into the *rcd2*-derived embryogenic calli via *Agrobacterium*-medi-

ated plant transformation. A total of 20 positive transformants were obtained and all of them displayed the normal green leaf phenotype similar to WT. In addition, the content of Chl of the complementation plants recovered to WT level (Figure 5(a,b)). Furthermore, we genotyped the complementary plants and confirmed the presence of the transgene manifested at the mutation site (Figure 5(c)). The results clearly demonstrated that *OsMH\_03G0040800* was the target gene responsible for the rapid cell death phenotype of *rcd2*.

We also performed the knockout of *OsMH\_03G0040800* to further validate its function under Kitaake genetic background, a total of 2 Kitaake-background knockout lines were obtained (Figure 5(d,e)). The knockout line *Cas9-2* had a six base deletion on the 4th exon (Figure 5(f)), resulting in the frameshift mutation. Unlike *rcd2*, *Cas9-2* exhibited similar reddish-brown lesions but more severe wilted leaf blades leading to seedling death. Based on the annotation at the NCBI databank, *RCD2* or *OsMH\_03G0040800* encodes a putative pheophorbide a oxygenase (PAO) and plays a vital role in Chl degradation in plants.

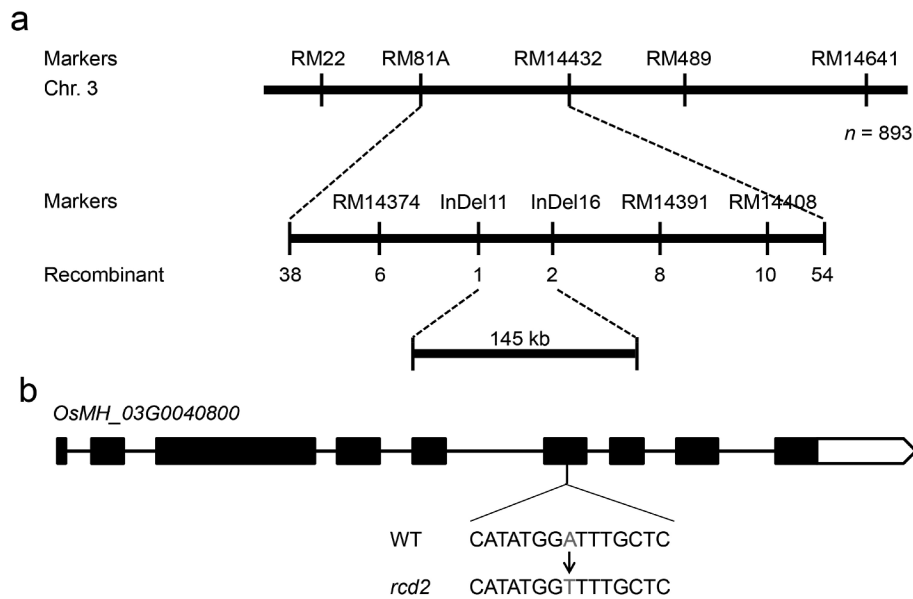


**Figure 4. Map-based cloning of *RCD2*.** (a) The mutation is delimited to a 145 kb region by genotyping 893 mutant type  $F_2$  individuals from the cross *rcd2*/80A90YR72; (b) sequence analysis reveals a single nucleotide substitution from A to T in the 6th exon of *OsMH\_03G0040800*. Arrow head indicates the mutation site.

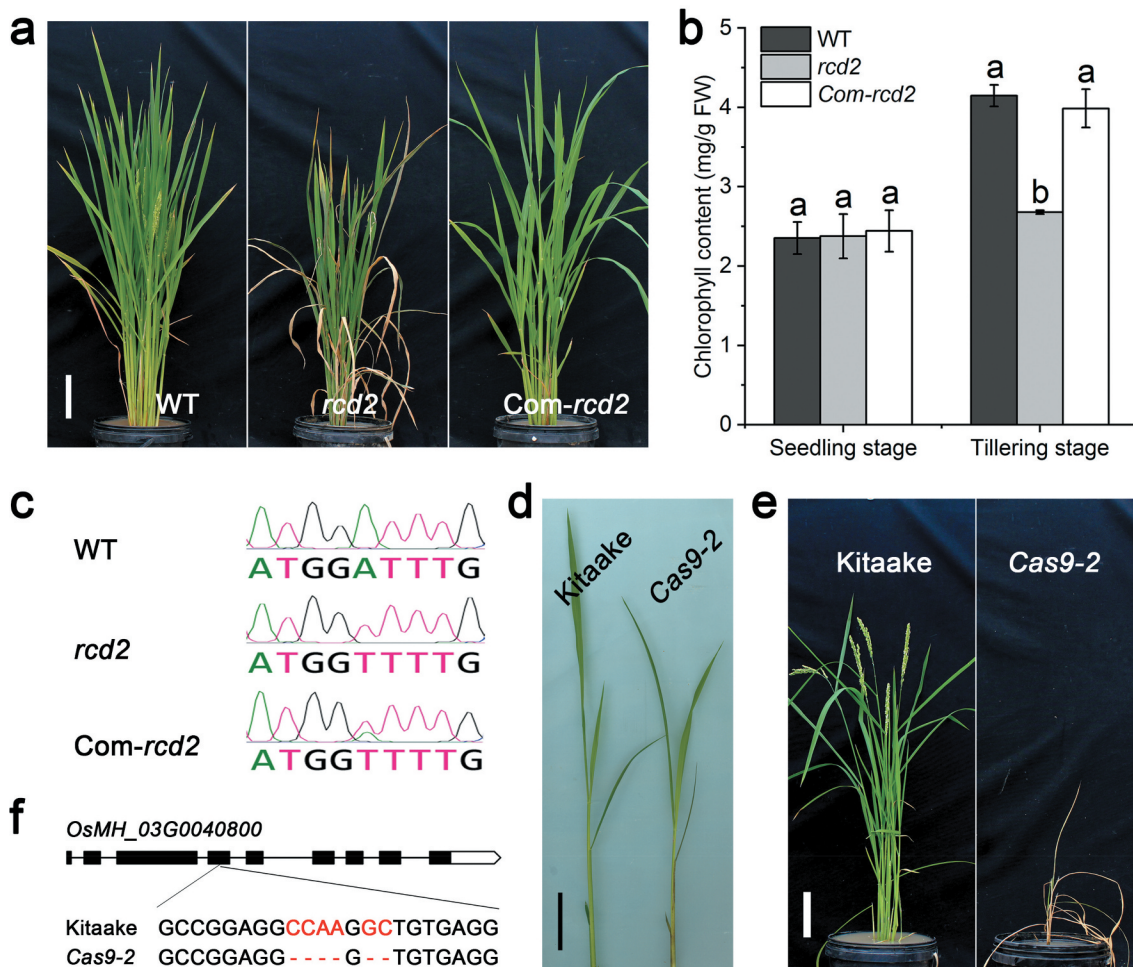


**Figure 5. Functional complementation of *rcd2*.** (a) Phenotype of WT, *rcd2*, and complementation line (Com-*rcd2*). Bar = 10 cm; (b) Chl contents of wild type, *rcd2* and complementation line. Values are means  $\pm$  SD ( $n = 3$ ). Different letters indicate significant differences by one-way ANOVA and Duncan's test ( $P < .05$ ); (c) sequencing analysis of WT, *rcd2* and complementation line; (d) phenotype of Kitaake and Kitaake PAO-knockout line (*Cas9-2*) at four-leaf stage; Bar = 5 cm; (e) phenotype of Kitaake and *Cas9-2* at the heading stage; (f) sequencing analysis of Kitaake and knockout line *Cas9-2* that shows a 6 bp deletion in the fourth exon of *PAO*.

### Enzymatic activities, intermediate contents and expression of Chl-metabolism-associated genes

Having known that *RCD2* encoded a PAO, we then carried out PAO activity assay, PAO content and substrate measurements. The results showed that both the activity and content of PAO were significantly decreased in *rcd2* compared with WT (Figure 6(a,b)). In contrast, the level of Pheide a, the substrate of PAO, was apparently increased in *rcd2* compared with WT (Figure 6(c)). Pheide a is a phototoxic substance whose accumulation could destroy the mesophyll cells in light, leading to the lesion formation. Taken together, our results suggested that the I576F mutation lead to impaired function of PAO and the accumulation of Pheide a in *rcd2*.

To determine the mutation effects on the expression of relevant genes and enzymatic activities in the PAO pathway, we performed qRT-PCR and ELISA analysis, respectively, on eight genes (*PAO*, *RCCR1*, *SGR*, *NYC3*, *CLH*, *SGRL* and *CLHS*) associated with Chl degradation, and two genes (*CAO1* and *CAO2*) associated with Chl biosynthesis. Our results showed that the expressions of *PAO*, *RCCR1*, *SGR*, *NYC3*, *CLH*, *SGRL* and *CAO1* were apparently downregulated, while the expression of *CLHS* was significantly upregulated in *rcd2* at the late tillering stage compared with WT. The expression of *CAO2* was similar between *rcd2* and WT (Figure 6(d)). In addition, the accumulation of Chlide a, the product of CLH, and Phein a, the substrate of PPH, were significantly increased in *rcd2* compared with WT (Figure 6(e,f)), suggesting that CLH

might play a role in Chl degradation. Interestingly, the activity of CLH was apparently decreased in *rcd2* although the level of Chlide a was increased (Figure 6(g)). Furthermore, the activities of RCCR and MDCase (*SGR*) were apparently increased while the activity of PPH was similar between *rcd2* and WT (Figure 5(h-j)). Nevertheless, the results indicated that the mutation impaired the expression of nearly all genes associated with Chl degradation.

### Altered enzymatic activities, intermediate contents and gene expression in dark

To determine the effect of darkness on the enzymatic activities, intermediate contents and expression of Chl metabolism-associated genes, we carried out analysis on the detached WT and *rcd2* leaves without lesions at the early tillering stage. The results showed that the expression of *PAO*, *RCCR1*, *SGR* and *CLHS* were greatly upregulated, and the expressions of *NYC3*, *SGRL* and *CAO1* were apparently downregulated in *rcd2* compared with WT while the expression of *CAO2* and *CLH* was similar between *rcd2* and WT before dark treatment (Figure 7(a)). Furthermore, the PAO content and activity in *rcd2* were significantly lower than those of WT before dark treatment (Figure 7(c, d)). The level of Pheide a in *rcd2* was apparently higher than that of WT before dark treatment (Figure 7(e)). The levels of Chlide a and Phein a were similar between *rcd2* and WT before dark treatment (Figure 7(f,g)). The activity of CLH decreased obviously, and the

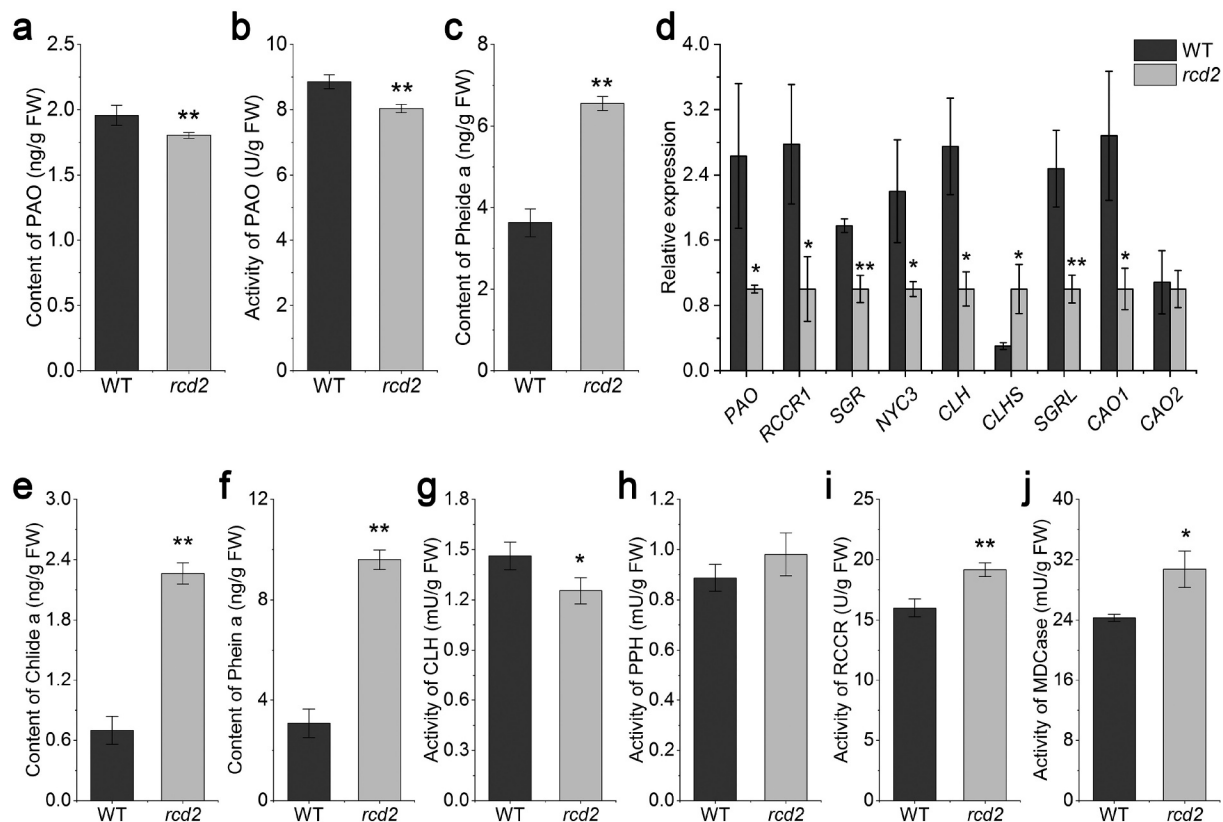


**Figure 6. Analysis of enzymatic activities, intermediate content and expression of relevant genes-associated with Chl metabolism.** (a) PAO content, (b) PAO activity and (c) Pheide a content of WT and *rcd2* at the late tillering stage; (d) expression profile of relevant Chl metabolism genes in WT and *rcd2* after lesion appeared; (e) Chlide a content; (f) Phein a content; (g-j) activities of CLH, PPH, RCCR and MDCase. Values are means  $\pm$  SD;  $n = 3$ ; \* indicates significance at  $P < .05$ ; \*\* indicates significance at  $P < .01$  by Student's *t*-test. The top second leaves at the late tillering stage were used for analysis in all experiments.

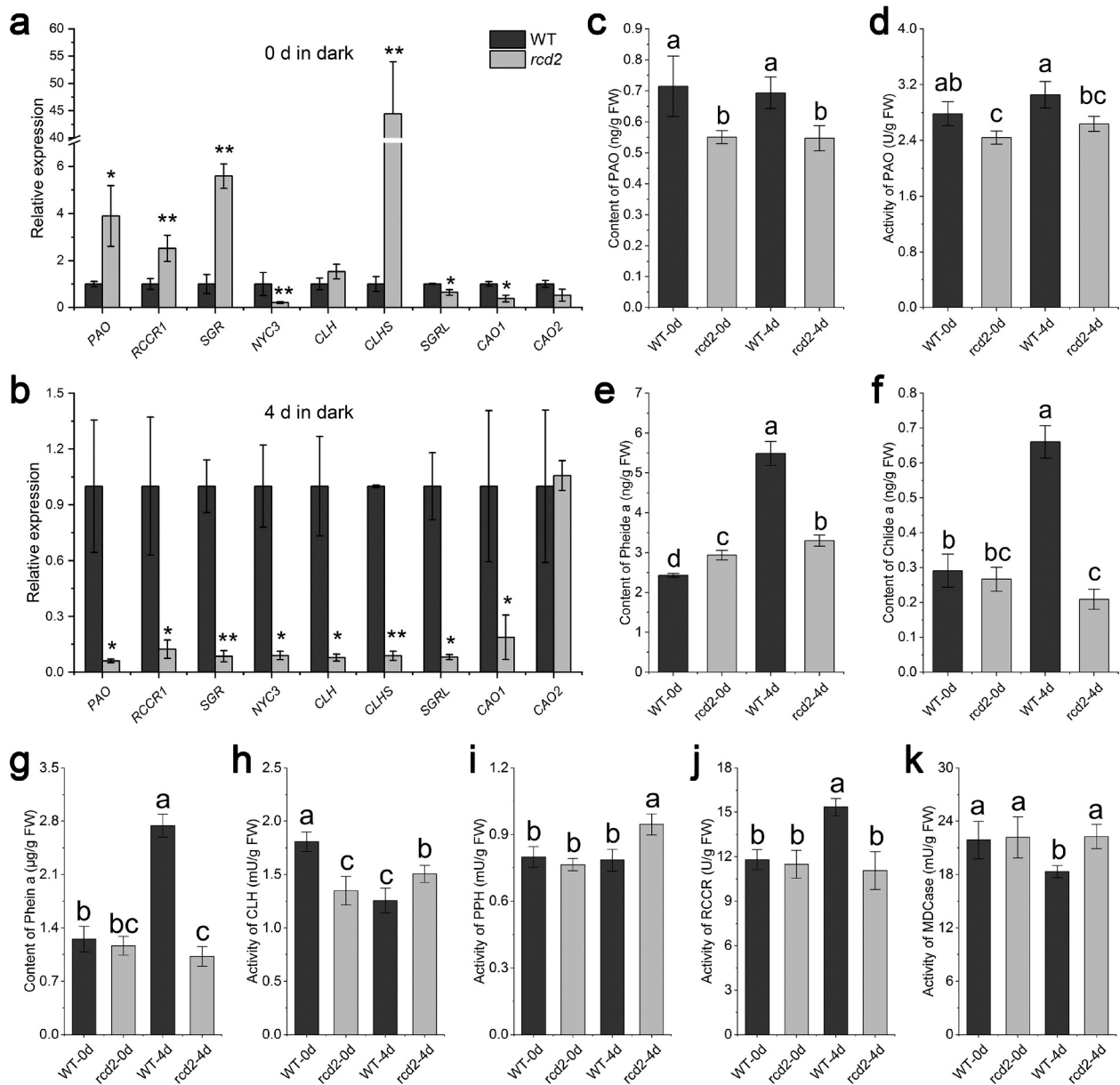


**Figure 7. Analysis of enzymatic activities, intermediate contents and Chl metabolism-related genes after dark treatment.** (a,b) Gene expression profile in detached leaves of WT and *rcd2* without lesions at 0 d and 4 d dark treatment. Values are means  $\pm$  SD;  $n=3$ ; \*\* indicates significance at  $P \leq 0.01$  by Student's *t*-test; (c-e) PAO content, PAO activity and Pheide a contents of WT and *rcd2* leaves without lesions at 0 d and 4 d dark treatment; (f,g) Chlide a and Phein a contents of WT and *rcd2* leaves without lesions at 0 d and 4 d dark treatment; (h-k) activities of CLH, PPH, RCCR and MDCase of WT and *rcd2* leaves without lesions at 0 d and 4 d dark treatment. Values are means  $\pm$  SD ( $n=3$ ). Different letters indicate significant differences by one-way ANOVA and Duncan's test ( $P < .05$ ); The top second leaves without lesions at the early tillering stage were used for analysis in all experiments.

activities of PPH, RCCR and MDCase were similar between *rcd2* and WT before dark treatment (Figure 7(h–k)). The results indicated that the mutation affected Chl metabolism-associated gene expression before lesion formation.

After 4d dark treatment, the expressions of *PAO*, *RCCR1*, *SGR*, *NYC3*, *CLH*, *SGRL*, *CLHS* and *CAO1* were significantly down-regulated in *rcd2* compared with WT except *CAO2* which was similar between the two genotypes (Figure 7(b)). In addition, the level and activity of PAO were significantly decreased in *rcd2* compared to WT (Figure 5(c,d)). The levels of Pheide a, Chlide a and Phein a were apparently lower than those of WT (Figure 7(e–g)). The activities of CLH, PPH and MDCase were increased obviously and the activity of RCCR1 was apparently decreased in *rcd2* compared with WT (Figure 7(h–k)). Our results demonstra

ted that dark treatment inhibited significantly the expression of Chl metabolism-associated genes in the *PAO* pathway and retarded Chl degradation, leading to the stay-green phenotype in *rcd2*.

## Discussion

Cell death mutants have been widely reported in a number of plant species. These mutants usually produce necrotic leaf lesions similar to those caused by hypersensitive response (HR), a type of programmed cell death (PCD) induced by pathogen invasion.<sup>28</sup> A group of cell death mutant is associated with deficiencies in the *PAO* pathway. For example, the Arabidopsis-accelerated cell death (*acd2*) mutant generates lesion mimic phenotype resulting from

a mutation in *ACD2* that encodes a red chlorophyll catabolite reductase.<sup>29</sup> In the present study, we identified a *rapid cell death* mutant *rcd2* and isolated the responsible gene *RCD2* encoding pheophorbide a oxygenase, the key enzyme in the PAO pathway. The PAO proteins are highly conserved in plants. Substitution of any amino acid residue would result in impaired functions of the enzyme. For example, the T255I in EAS1 disrupted the PAO activity and function in rice.<sup>9</sup> In our case, the isoleucine at position 576 is also highly conserved and its substitution by phenylalanine resulted in decreased activity and content of PAO.

Like many cell death mutants or lesion mimic mutant with cell death,<sup>30–32</sup> *rcd2* leaves undergo a series of biochemical/physiological changes such as decreased chlorophyll and soluble protein content, increased MDA content and declined photosynthetic capacity. Besides, *rcd2* also exhibited accumulation of ROS and altered activities of ROS scavenging enzymes including CAT, POD and SOD. In plants, the excessive amount of ROS is thought to be the cause for necrotic leaf lesions, but which type of ROS responsible for cell death varies. For example, the rapid ROS production generated from the accumulation of Pheide a in Arabidopsis *acd1* is responsible for the propagation of cell death.<sup>7</sup> In sorghum *dead1*, the lack of superoxide and H<sub>2</sub>O<sub>2</sub> production in/around lesions suggests these two ROSs are not responsible for lesion formation; instead, singlet oxygen (<sup>1</sup>O<sub>2</sub>) derived from Pheide a might be the direct cause but has yet to be clarified.<sup>10</sup> In the present study, the accumulation of O<sub>2</sub><sup>-</sup> rather than H<sub>2</sub>O<sub>2</sub> is likely responsible for the rapid cell death in *rcd2*.

In plants, phototoxic substances are responsible for necrotic lesions of some mutants associated with the defective in PAO or the PAO pathway, such as Pheide a of *lls1* in maize and Pheide a of *acd1* in Arabidopsis and RCC of *acd2* in Arabidopsis. In Arabidopsis, *acd2* develops a cell death phenotype which highly correlates with the accumulation of RCC and RCC-like pigments.<sup>33</sup> In *rcd2*, we found similar necrotic lesions and the increased level of Pheide a due to the significantly decreased gene expression, activity and content of PAO. The lesion formation is also light-dependent, suggesting that the accumulation of Pheide a could damage the mesophyll cells in light and lead to the lesion formation in *rcd2*. Furthermore, some PAO pathway-defective mutants such as Arabidopsis *pph-1* and rice *NYC3*<sup>34,35</sup> show “stay-green” phenotype due to the breakdown of Chl degradation. In the present study, *rcd2* also showed a “stay-green” phenotype after dark treatment, suggesting the mutation of *RCD2* delayed the degradation of chlorophylls in dark.

So far, the role of *CLHs* in Chl degradation is controversial. In the present study, *rcd2* displayed significantly increased accumulation of Pheide a, which was derived from Chl after the removal of Mg<sup>++</sup> and would be dephytylated by pheophytin pheophorbide hydrolase (pheophytinase, PPH) in Arabidopsis or non-yellow coloring 3 (*NYC3*) in rice.<sup>34–36</sup> Pheide a, the certain intermediate metabolite of Chl degradation, was highly accumulated in the detached senescent leaves of WT after 4 d dark treatment, suggesting that PPH played a vital role for Chl degradation. Interestingly, we also observed apparent accumulation of Chlide a, a product from Chl by the catalysis of *CLHs*, implying that Chlide a may also be an intermediate metabolite of Chl degradation in dark. This was supported by the upregulated expression of chlorophyllase gene *CLHS*, which can hydrolyze Chl to Chlide. Unexpected

ly, the activity of *CLHs* was apparently increased in *rcd2* although the level of Chlide a was decreased compared with WT after 4d dark treatment, suggesting that over-accumulation of Chlide a might feedback inhibited the activity of *CLHs*. Therefore, we assumed that *CLHs* might involve in senescence-related Chl degradation in rice although further validation by knockout of *CLHs*-related genes would be helpful.

In conclusion, the A1726T mutation of the key gene *PAO* in the Chl degradation pathway could seriously impact the normal growth and reproduction in rice. The accumulation of O<sub>2</sub><sup>-</sup> instead of H<sub>2</sub>O<sub>2</sub> in *rcd2* could be the direct cause for the lesion formation in *rcd2*. Furthermore, *CLHs* might play a role in Chl degradation in rice.

## Author contributions

Conceptualization, ZZ and J-LW; Investigation, ZZ, YH, LL, YS, XX, and XZ; Supervision, J-L W; Writing – original draft, Z Z; Writing – review & editing, J-LW.

## Disclosure of Potential Conflicts of Interest

The authors declare no conflict of interest.

## Funding

This research was funded by the Central Public-interest Scientific Institution Basal Research Fund of China National Rice Research Institute (2017RG002-2).

## ORCID

Jian-Li Wu  <http://orcid.org/0000-0003-3480-1503>

## References

- Ding Y, Wu G, Guo CK. Research advance on chlorophyll degradation in plants. *Biotech Bull.* 2016;32:1–9. (in Chinese with English abstract).
- Hörtensteiner S. Update on the biochemistry of chlorophyll breakdown. *Plant Mol Biol.* 2013;82:505–517. doi:10.1007/s11103-012-9940-z.
- Benke K, Chen JY, Hörtensteiner S. The biochemistry and molecular biology of chlorophyll breakdown. *J Exp Bot.* 2018;69:751–767.
- Spasieva S, Hille J. A lesion mimic phenotype in tomato obtained by isolating and silencing an *lls1* homologue. *Plant Sci.* 2002;162:543–549. doi:10.1016/S0168-9452(01)00595-7.
- Pružinská A, Tanner G, Anders I, Roca M, Hörtensteiner S. Chlorophyll breakdown: pheophorbide a oxygenase is a Rieske-type iron-sulfur protein, encoded by the *accelerated cell death 1* gene. *Proc Natl Acad Sci USA.* 2003;100:15259–15264. doi:10.1073/pnas.2036571100.
- Tanaka R, Hirashima M, Satoh S, Tanaka A. The *Arabidopsis*-accelerated cell death gene *ACD1* is involved in oxygenation of pheophorbide a: inhibition of the pheophorbide a oxygenase activity does not lead to the “stay-green” phenotype in Arabidopsis. *Plant Cell Physiol.* 2003;44:1266–1274. doi:10.1093/pcp/pcg172.
- Yang M, Wardzala E, Johal GS, Gray J. The wound-inducible *Lls1* gene from maize is an orthologue of the Arabidopsis *Acd1* gene, and the *LLS1* protein is present in non-photosynthetic tissues. *Plant Mol Biol.* 2004;54:175–191. doi:10.1023/B:PLAN.0000028789.51807.6a.
- Tang C, Wang X, Duan X, Wang X, Huang L, Kang Z. Functions of the *lethal leaf-spot 1* gene in wheat cell death and disease tolerance to *Puccinia striiformis*. *J Exp Bot.* 2013;64:2955–2969. doi:10.1093/jxb/ert135.

9. Xie QJ, Liang Y, Zhang J, Zheng HK, Dong GJ, Qian Q, Zuo JR. Involvement of a putative bipartite transit peptide in targeting rice pheophorbide a oxygenase into chloroplasts for chlorophyll degradation during leaf senescence. *J Genet Genomics*. 2016;43:145–154. doi:10.1016/j.jgg.2015.09.012.
10. Sindhu A, Janick-Buckner D, Buckner B, Gray J, Zehr U, Dilkes BP, Johal GS. Propagation of cell death in *dropdead1*, a sorghum ortholog of the maize *lls1* mutant. *PLoS ONE*. 2018;13:e0201359. doi:10.1371/journal.pone.0201359.
11. Tang L. Pheophorbide a monooxygenase and chlorophyll degradation. *Chem Life*. 2008;28:606–609. (in Chinese with English abstract).
12. Gray J, Janick-Buckner D, Buckner B, Close PS, Johal GS. Light-dependent death of maize *lls1* cells is mediated by mature chloroplasts. *Plant Physiol*. 2002;130:1894–1907. doi:10.1104/pp.008441.
13. Takamiya K, Tsuchiya T, Ohta H. Degradation pathway(s) of chlorophyll: what has gene cloning revealed? *Trends Plant Sci*. 2000;5:426–431. doi:10.1016/S1360-1385(00)01735-0.
14. Harpaz-Saad S, Azoulay T, Arazi T, Ben-Yaakov E, Mett A, Shibolet Y, Hörtensteiner S, Gidoni D, Gal-On A, Goldschmidt EE, et al. Chlorophyllase is a rate-limiting enzyme in chlorophyll catabolism and is posttranslationally regulated. *Plant Cell*. 2007;19:1007–1022. doi:10.1105/tpc.107.050633.
15. Hörtensteiner S. Chlorophyll degradation during senescence. *Annu Rev Plant Biol*. 2006;57:55–57. doi:10.1146/annurev.arplant.57.032905.105212.
16. Schenk N, Schelbert S, Kanwischer M, Goldschmidt EE, Dörmann P, Hörtensteiner S. The chlorophyllases *AtCLH1* and *AtCLH2* are not essential for senescence-related chlorophyll breakdown in *Arabidopsis thaliana*. *FEBS Lett*. 2007;581:5517–5525. doi:10.1016/j.febslet.2007.10.060.
17. Chen LFO, Lin CH, Kelkar SM, Chang YM, Shaw JF. Transgenic broccoli (*Brassica oleracea* var. *italica*) with antisense chlorophyllase (*BoCLH1*) delays postharvest yellowing. *Plant Sci*. 2008;174:25–31. doi:10.1016/j.plantsci.2007.09.006.
18. Azoulay ST, Harpaz-Saad S, Belausov E, Lovat N, Krokhin O, Spicer V, Standing KG, Goldschmidt EE, Eyal Y. Citrus chlorophyllase dynamics at ethylene-induced fruit color-break; a study of chlorophyllase expression, post-translational processing kinetics and in-situ intracellular localization. *Plant Physiol*. 2008;148:108–118. doi:10.1104/pp.108.124933.
19. Thordal-Christensen H, Zhang ZG, Wei YD, Collinge DB. Subcellular localization of H<sub>2</sub>O<sub>2</sub> in plants: H<sub>2</sub>O<sub>2</sub> accumulation in papillae and hypersensitive response during the barley-powdery mildew interaction. *Plant J*. 1997;11:1187–1194. doi:10.1046/j.1365-3113.1997.11061187.x.
20. Yin ZC, Chen J, Zeng LR, Goh M, Leung H, Khush GS, Wang GL. Characterizing rice lesion mimic mutants and identifying a mutant with broad-spectrum resistance to rice blast and bacterial blight. *Mol Plant Microbe Interact*. 2000;13:869–876. doi:10.1094/MPMI.2000.13.8.869.
21. Qiao YL, Jiang WZ, Lee JH, Park BS, Choi MS, Piao RH, Woo MO, Roh JH, Han LZ, Paek NC, et al. SPL28 encodes a clathrin-associated adaptor protein complex 1, medium subunit  $\mu$ 1 (AP1M1) and is responsible for spotted leaf and early senescence in rice (*Oryza sativa*). *New Phytol*. 2010;185:258–274. doi:10.1111/j.1469-8137.2009.03047.x.
22. Edwards K, Johnstone C, Thompson C. A simple and rapid method for the preparation of plant genomic DNA for PCR analysis. *Nucl Acids Res*. 1991;19:1349. doi:10.1093/nar/19.6.1349.
23. Ma X, Zhang Q, Zhu Q, Liu W, Chen Y, Qiu R, Wang B, Yang Z, Li H, Lin Y, et al. A robust CRISPR/Cas9 system for convenient, high-efficiency multiplex genome editing in monocot and dicot plants. *Mol Plant*. 2015;8:1274–1284. doi:10.1016/j.molp.2015.04.007.
24. Hiei Y, Komari T. Agrobacterium-mediated transformation of rice using immature embryos or calli induced from mature seed. *Nat Protoc*. 2008;3:824–834. doi:10.1038/nprot.2008.46
25. Huang QN, Yang Y, Shi YF, Chen J, Wu JL. Spotted-leaf mutants of rice (*Oryza sativa*). *Rice Sci*. 2010;17:247–256. doi:10.1016/S1672-6308(09)60024-X.
26. Kong Z, Li M, Yang W, Xu W, Xue Y. A novel nuclear-localized CCCH-type zinc finger protein, OsDOS, is involved in delaying leaf senescence in rice. *Plant Physiol*. 2006;141:1376–1388. doi:10.1104/pp.106.082941.
27. Liu H, Wang Y, Xu J, Su T, Liu G, Ren D. Ethylene signaling is required for the acceleration of cell death induced by the activation of AtMEK5 in Arabidopsis. *Cell Res*. 2008;18:422–432. doi:10.1038/cr.2008.29.
28. Walbot V, Hoisington DA, Neuffer MG. Disease lesion mimic mutations. In: Kosuge T, et al (eds) . *Genetic Engineering of Plants*. Plenum Press, New York.; 1983, pp431-442.
29. Mach JM. The Arabidopsis-accelerated cell death gene *ACD2* encodes red chlorophyll catabolite reductase and suppresses the spread of disease symptoms. *Proc Natl Acad Sci USA*. 2001;98:771–776. doi:10.1073/pnas.98.2.771.
30. Chen Z, Chen T, Sathe AP, He YQ, Zhang XB, Wu JL. Identification of a novel semi-dominant spotted-leaf mutant with enhanced resistance to *Xanthomonas oryzae* pv. *oryzae* in rice. *Int J Mol Sci*. 2018;19:3766. doi:10.3390/ijms19123766.
31. Feng BH, Yang Y, Shi YF, Shen HC, Wang HM, Huang QN, Xu X, Lü XG, Wu JL. Characterization and genetic analysis of a novel rice spotted-leaf mutant *HM47* with broad-spectrum resistance to *Xanthomonas oryzae* pv. *oryzae*. *J Integr Plant Biol*. 2013;55:473–483. doi:10.1111/jipb.12021.
32. He Y, Zhang ZH, Li LJ, Tang SQ, Wu JL. Genetic and physio-biochemical characterization of a novel premature senescence leaf mutant in rice (*Oryza sativa* L.). *Int J Mol Sci*. 2018;19:2339. doi:10.3390/ijms19082339.
33. Pružinská A, Anders I, Aubry S, Schenk N, Tapernoux-Lüthi E, Müller T, Krätler B, Hörtensteiner S. In vivo participation of red chlorophyll catabolite reductase in chlorophyll breakdown. *Plant Cell*. 2007;19:369–387. doi:10.1105/tpc.106.044404.
34. Schelbert S, Aubry S, Burla B, Agne B, Kessler F, Krupinska K, Hörtensteiner S. Pheophytin pheophorbide hydrolase (pheophytinase) is involved in chlorophyll breakdown during leaf senescence in Arabidopsis. *Plant Cell*. 2009;21:767–785. doi:10.1105/tpc.108.064089.
35. Shimoda Y, Ito H, Tanaka A. Arabidopsis STAY-GREEN, Mendel's green cotyledon gene, encodes magnesium-dechelataase. *Plant Cell*. 2016;28:2147–2160. doi:10.1105/tpc.16.00428.
36. Morita R, Sato Y, Masuda Y, Nishimura M, Kusaba M. Defect in non-yellow coloring 3, an  $\alpha/\beta$  hydrolase-fold family protein, causes a stay-green phenotype during leaf senescence in rice. *Plant J*. 2009;59:940–952. doi:10.1111/j.1365-3113.2009.03919.x.